



## Short communication

## Investigation on the performance evaluation method of flow batteries



Qiong Zheng<sup>a,b,c</sup>, Feng Xing<sup>a</sup>, Xianfeng Li<sup>a</sup>, Tao Liu<sup>a</sup>, Qinzhi Lai<sup>a</sup>, Guiling Ning<sup>b,\*</sup>,  
Huamin Zhang<sup>a,\*</sup>

<sup>a</sup> Division of Energy Storage, Dalian Institute of Chemical Physics, Chinese Academy of Sciences, Dalian 116023, PR China

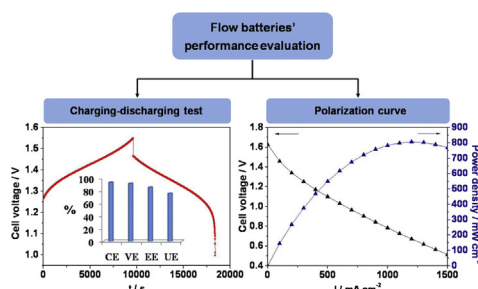
<sup>b</sup> School of Chemical Engineering, Dalian University of Technology, Dalian 116023, PR China

<sup>c</sup> Graduate University of the Chinese Academy of Sciences, Beijing 100039, PR China

## HIGHLIGHTS

- A proper performance evaluation method for flow batteries is very important.
- Polarization curve is not advisable to evaluate flow batteries' performance.
- Charging–discharging test is optimal for flow batteries' performance evaluation.

## GRAPHICAL ABSTRACT



## ARTICLE INFO

## Article history:

Received 23 January 2014

Received in revised form

27 March 2014

Accepted 30 April 2014

Available online 14 May 2014

## Keywords:

Performance evaluation method

Flow batteries

Charging–discharging test

Polarization curve

## ABSTRACT

Performance evaluation method is very important for the research on flow batteries. Charging–discharging test is the most typical evaluation method for flow batteries. Recently, the polarization curves, together with the associated power density curves, which are commonly employed in fuel cells, have come into use for flow batteries' performance evaluation. Based on the investigation of performance evaluation method, it is confirmed charging–discharging test is optimal for flow batteries' performance evaluation. A comparison of voltage losses (voltage efficiency, VE) can be clearly delivered from the polarization curves, which are quite practical for fuel cells' performance evaluation. While for flow batteries, apart from VE, coulombic efficiency (CE), energy efficiency (EE), utilization of electrolyte (UE) and capacity stability should be seriously considered during charging–discharging process. However, CE and UE are inaccessible; accordingly EE and capacity stability can't be detected from polarization curves. Therefore, the polarization curve is improper to serve as a performance evaluation method for flow batteries. On the premise of a proper CE, a rough performance evaluation for flow batteries can be achieved via the polarization curves. The peak power density is of limited significance in practical use due to the extremely low EE obtained at that point.

© 2014 Elsevier B.V. All rights reserved.

## 1. Introduction

Flow batteries are considered among the most promising technologies for large-scale energy storage due to their attractive

features like long cycle life, high efficiency and high reliability [1–3]. A large number of flow batteries have been successively proposed and developed, such as all-vanadium [4], iron–chromium [5], bromine–polysulfide [6] and zinc–bromine [7]. Meanwhile, some relevant experimental and modeling studies have been performed to improve the battery performance through material innovation and structure optimization [8–15]. Therefore to achieve the reliable and comparable battery performance is essential, and a

\* Corresponding authors.

E-mail addresses: [ninggi@dlut.edu.cn](mailto:ninggi@dlut.edu.cn) (G. Ning), [zhanghm@dicp.ac.cn](mailto:zhanghm@dicp.ac.cn) (H. Zhang).

proper performance evaluation method for flow batteries is of great importance.

Currently, the most typical and commonly used performance evaluation method for flow batteries is charging–discharging test, mainly indicating four characteristics: (1) Coulombic efficiency (CE), the ratio of the average discharging capacity to the average charging capacity, (2) Voltage efficiency (VE), the ratio of the average discharging voltage to the average charging voltage, (3) Energy efficiency (EE), the ratio of the average discharging energy to the average charging energy, (4) Utilization of electrolyte (UE), the ratio of the actual discharging capacity to the theoretical discharging capacity. In addition, capacity fading, evaluated by plotting UE with respect to cycle number, is an indicator of capacity stability of flow batteries during charging–discharging cycling.

The polarization curves and the associated power density curves, which were widely used for performance evaluation of fuel cells [16,17], have recently come into use for flow batteries' performance evaluation [18–22]. The battery performance was improved via lowering the polarization and enhancing the peak power density by using this method. The polarization curves describe the output voltage at the specified current density, by which the mechanism of voltage losses can be extensively studied and the detailed research has been reported in Ref. [23]. And the power density curves are derived from the product of the output voltage and the corresponding current density.

Different from fuel cells, the flow batteries are rechargeable, where the overall performance is closely related to the charging–discharging process. However, the polarization curves can only identify the mechanism of the voltage losses; therefore it is necessary to access the availability of this method for performance evaluation and to clarify the issues that the polarization curves could address for flow batteries.

In this communication, membranes with different thicknesses were selected to further tune the internal resistance of batteries. The charging–discharging test and the polarization curves were presented respectively to evaluate the performance of flow batteries with different internal resistances. The performance consistence between the two methods was investigated. The feasibility of using polarization curves for flow batteries' performance evaluation was discussed.

## 2. Experimental

### 2.1. Battery construction and electrolyte system

As shown in Fig. 1, a vanadium flow battery (VFB), comprised of a membrane, electrodes (installed in the frames), frames and current

collectors, was assembled for battery performance evaluation. Nafion-series with different thickness were used as membranes, including Nafion 115 (125  $\mu\text{m}$ ), 212 (50  $\mu\text{m}$ ) and 211 (25  $\mu\text{m}$ ) (Ion-Power, Inc.). The electrodes were carbon felts with an original thickness of 1 mm and a geometric surface area of 6.72  $\text{cm}^2$ . Seals with a hollow area of 6.72  $\text{cm}^2$  served as the frames, where the electrodes were installed. The frames filled with electrodes and the membrane, were mounted by sandwiching between current collectors (graphite plates). The battery was assembled with gaskets suitable to compress the electrode material to a rough 80% of its original thickness. 40 mL of a solution containing 1.5 M  $\text{VO}^{2+}$ , 3 M  $\text{H}_2\text{SO}_4$  and 40 mL of a solution containing 1.5 M  $\text{V}^{3+}$ , 3 M  $\text{H}_2\text{SO}_4$  were used as positive and negative electrolyte, respectively.

### 2.2. Battery measurements

The charging–discharging test was conducted by an Arbin 2000 instrument at the current density ranging from 80  $\text{mA cm}^{-2}$  to 200  $\text{mA cm}^{-2}$ . The polarization curve was generally measured by controlled current-steady steps using a FC Impedance Meter (KFM 2030) with a maximum current of 30 A. A steady current below 2  $\text{mA cm}^{-2}$  at a charging voltage of 1.75 V was taken to indicate 'fully charged' state of the electrolyte, consisting of  $\text{V}^{2+}$  on the negative side and  $\text{V}^{5+}$  on the positive side. The discharging polarization curve, started with the battery at 'fully charged' state, was studied. The battery was discharged at the specified current density for 30 s and then allowed to rest for up to a steady state at its open circuit voltage (OCV). The internal resistance (IR) of the battery was measured during the polarization curve test at 'fully charged' state by the aforementioned FC Impedance Meter.

All experiments were performed at room temperature (25  $^{\circ}\text{C}$ ). Two centrifugal pumps were used to deliver electrolytes through the battery at a constant flow rate of 15  $\text{mL min}^{-1}$ . A PTFE sealing component was sealed onto the negative reservoir to avoid oxidation of  $\text{V}^{2+}$ . The cutoff voltage for charging–discharging test was set at 1.55 V and 1 V to avoid the corrosion of carbon felt and graphite plate.

## 3. Results and discussion

### 3.1. Charging–discharging performance

A typical plot of charging–discharging voltage versus time is shown in Fig. 2, which is a fundamental description on the battery performance during charging–discharging process. Referring to Fig. 2(a), a raise in charging voltage and a decline in discharging

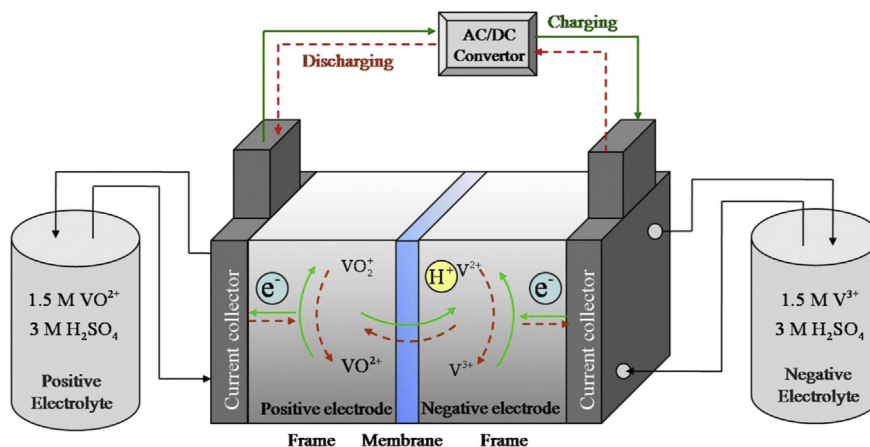
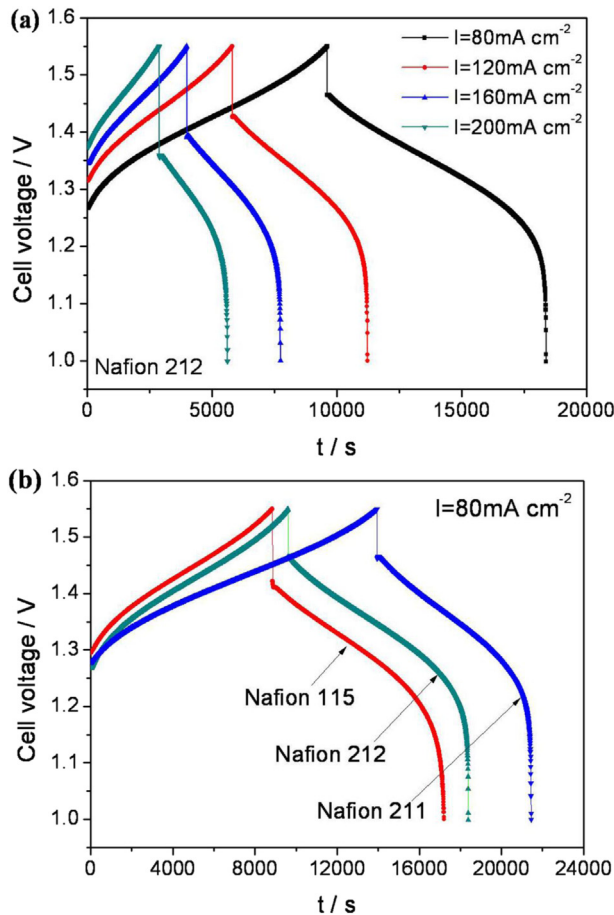


Fig. 1. Scheme of battery construction.



**Fig. 2.** (a) Charging–discharging voltage curves at different current densities for Nafion 212, (b) charging–discharging voltage curves of different membranes at the current density of  $80 \text{ mA cm}^{-2}$ .

voltage along with a reduced charging–discharging time are detected in accordance with increasing current densities, which is mainly caused by the increased voltage losses along with the elevated current densities. Based on the above definition, the relative CE, VE and UE for batteries assembled with different membranes can be roughly identified from Fig. 2(b) via the ratio of

the discharging time and charging time, the ratio of the average discharging voltage and charging voltage, and the discharging time, respectively. More detailed information of charging–discharging characteristics is given in Table 1.

As shown in Table 1, for the same membrane, there is simultaneous rise in CE and decline in VE along with the increase of current density. Normally, the former can be attributed to the much lower vanadium ions permeate rate than that of protons [11], more importantly, a reduced charging–discharging time at high current densities. The latter is caused by the increased voltage losses with elevated current densities. Meanwhile, the decrement of active materials available for electrochemical reactions with increased current densities leads to the decrease of UE. However, there is a distinct presence in EE, which is a combination of CE and VE. For Nafion 115 and 212, the rapid drop in VE is not offset by the small increase in CE, therefore resulting in an overall decrease of EE along with the increase of current density. While for Nafion 211 (the thinnest membrane), as the current density increases, a rapid raise in CE resulted from a significant reduction of vanadium ions crossover (caused by the significant reduction of charging–discharging time) along with a relatively slow drop in VE leads to an increase of EE with the elevated current density. Comparing the batteries assembled with various membranes, the battery assembled with thinner membrane shows lower CE while higher VE at the same current density, which can be ascribed to more vanadium ions crossover and lower internal resistance for the battery with thinner membrane. Normally, there is an increased value of UE with the reduced thickness of membrane as a result of the increased discharging time, while it is not applicable for Nafion 211 due to the serious vanadium ions crossover through the membrane.

To further evaluate the capacity stability of flow batteries, a typical plot of UE versus charging–discharging cycle number at the current density of  $200 \text{ mA cm}^{-2}$  is shown in Fig. 3. As expected, a relatively stable performance with the aforementioned highest UE is achieved over 40 cycles for the battery assembled with Nafion 212. However, drastic capacity fading of Nafion 211 is observed due to the massive vanadium ions crossover during repetition charging–discharging cycling.

Based on the charging–discharging characteristic comparison for different membranes, the battery assembled with Nafion 212 exhibits an optimal charging–discharging performance with the highest efficiency of VE, EE, and UE, along with acceptable CE and stable capacity within the operation range in this paper.

**Table 1**

Charging–discharging characteristic of different membranes at the current densities ranging from  $80 \text{ mA cm}^{-2}$  to  $200 \text{ mA cm}^{-2}$  (CE, VE, EE and UE).

$I$ (current density)/ $\text{mA cm}^{-2}$	Charging–discharging characteristic	Membrane		
		Nafion 115 ( $IR = 470.22 \text{ m}\Omega \text{ cm}^2$ )	Nafion 212 ( $IR = 344.40 \text{ m}\Omega \text{ cm}^2$ )	Nafion 211 ( $IR = 249.82 \text{ m}\Omega \text{ cm}^2$ )
80	CE/%	94.61	91.25	53.75
	VE/%	90.45	94.31	94.70
	EE/%	85.58	86.06	50.91
	UE/%	79.38	81.87	69.98
120	CE/%	95.22	93.43	57.94
	VE/%	85.44	91.71	92.01
	EE/%	81.35	85.69	53.31
	UE/%	69.88	75.95	60.95
160	CE/%	95.63	94.61	65.04
	VE/%	80.78	89.29	89.85
	EE/%	77.25	84.48	58.43
	UE/%	57.60	70.24	57.13
200	CE/%	95.97	95.19	67.50
	VE/%	75.97	86.88	87.80
	EE/%	72.91	82.70	59.26
	UE/%	43.11	63.84	53.18

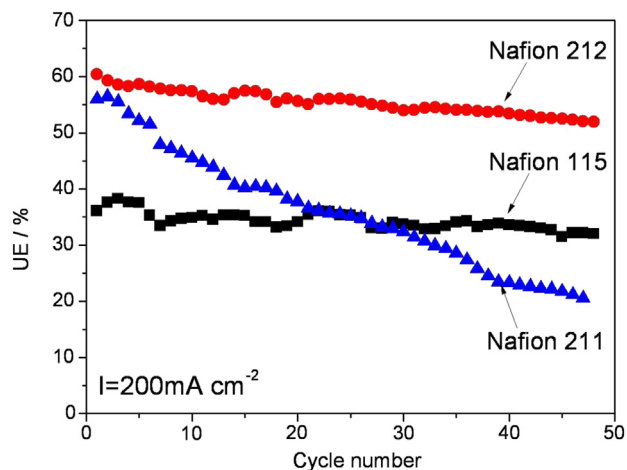


Fig. 3. Capacity stability of flow batteries assembled with different membranes during charging–discharging cycling at the current density of  $200 \text{ mA cm}^{-2}$ .

### 3.2. Polarization curve

On the other hand, the typical plot of polarization curves along with power density curves for flow batteries is shown in Fig. 4. Increased voltage losses can be observed with the elevated current densities, which is in accordance with the result in Fig. 2(a). In addition, there is a peak power density existing at a fairly high current density ( $>1000 \text{ mA cm}^{-2}$  in Fig. 4) for each battery. Comparing the results of flow batteries assembled with different membranes, the battery assembled with Nafion 211 presents the highest peak power density of  $1450.89 \text{ mW cm}^{-2}$  together with the least polarization due to the lowest internal resistance of Nafion 211, which is consistent with the highest voltage efficiency (VE) in Table 1. However, the extremely low values of CE ( $<70\%$ ) and EE ( $<60\%$ ) along with rapid drop in UE (70%) are detected at the current densities ranging from  $80 \text{ mA cm}^{-2}$  to  $200 \text{ mA cm}^{-2}$ , indicating a poor charging–discharging performance for Nafion 211. Even though a slight increment of polarization is observed for the battery with Nafion 212, the excellent charging–discharging performance with the encouraging energy efficiency (EE) generates a well comprehensive performance beyond that of the battery assembled with Nafion 211. Based on the analysis, the polarization curve is incapable of fully evaluating the charging–discharging performance for flow batteries.

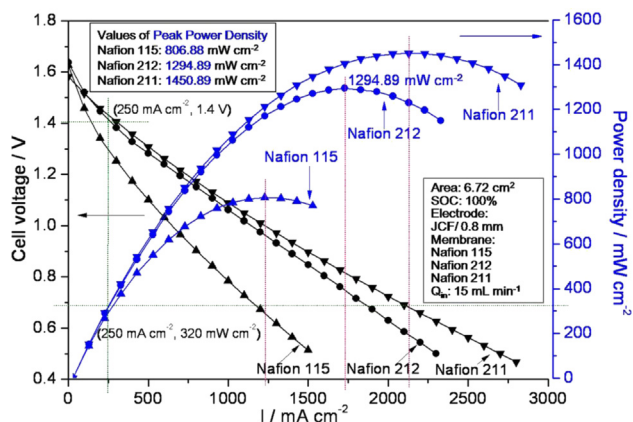


Fig. 4. Polarization curves and power density curves for the batteries assembled with various membranes.

This is assigned to that the polarization curve accounts for the mechanism of voltage losses and indicates directions for further improvement in the performance of the battery design [20]. Accordingly, a comparison of VE can be clearly delivered from the polarization curve, which is quite practical for fuel cells. While for flow batteries, CE, EE, UE and capacity stability should be seriously considered along with VE during charging–discharging process. However, CE and UE are inaccessible, and correspondingly EE and capacity stability can't be detected from the polarization curve. Therefore, the polarization curve is not advisable for flow batteries' performance evaluation.

Theoretically, on the premise of a proper CE, a rough performance evaluation and comparison for flow batteries can be achieved via the polarization curves and the power density curves. That is, for the battery assembled with Nafion 212, the performance with higher voltage ( $0.7617 \text{ V}$ ) and peak power density ( $1294.89 \text{ mW cm}^{-2}$ ) achieved at an acceptable CE (91%–97% for Nafion 115 and 212 in Table 1) is definitely better than that with Nafion 115 ( $0.6701 \text{ V}$ ,  $806.88 \text{ mW cm}^{-2}$ ). Within the practical operation range of a flow battery, such performance evaluation is also available for other conditions, such as different electrode materials [18], different battery structures [21].

To date, some demonstration projects of VFB system have been successfully implemented with energy efficiency (EE) of about 80% [24,25], which is expected to achieve the necessary cost structure for large-scale energy storage applications [26]. That is, the battery is not cost-effective and unpractical for large-scale energy storage at an extremely low value of EE. Taken Nafion 212 as an example, based on the criterion, at  $1.4 \text{ V}$  the battery's EE is about 80%. The practical maximum of current density is about  $250 \text{ mA cm}^{-2}$  and the practical power density is about  $320 \text{ mW cm}^{-2}$ , which is much lower than the peak power density of  $1294.89 \text{ mW cm}^{-2}$ . The analysis above indicates that an extremely low value of EE would be gained at the point of the peak power density, correspondingly which is of limited significance in practical use for flow batteries.

### 4. Conclusion

Performance evaluation is very important for the research on flow batteries. Based on the analysis, Charging–discharging test is the optimal performance evaluation method for flow batteries. The polarization curve can provide a comparison of VE by gaining an insight into the mechanism of voltage losses, whereas the CE and UE are inaccessible, and accordingly the EE and capacity stability can't be detected via the polarization curve. Therefore, the polarization curves can't fully evaluate the charging–discharging performance for flow batteries. On the premise of a proper and comparable CE, a rough performance evaluation and comparison for flow batteries can be achieved via the polarization curves. The peak power density is of limited significance in practical use due to an extremely low value of EE obtained at that point.

### Acknowledgment

Financial support from '973' project of MOST (Ministry of Science and Technology of China) (2010CB227205) is gratefully acknowledged.

### References

- [1] A.Z. Weber, M.M. Mench, J.P. Meyers, P.N. Ross, J.T. Gostick, Q. Liu, J. Appl. Electrochem. 41 (2011) 1137–1164.
- [2] M. Skyllas-Kazacos, M. Chakrabarti, S. Hajimolana, F. Mjalli, M. Saleem, J. Electrochem. Soc. 158 (2011) R55–R79.
- [3] P. Leung, X. Li, C.P. de León, L. Berlouis, C.J. Low, F.C. Walsh, RSC Adv. 2 (2012) 10125–10156.

- [4] E. Sum, M. Rychcik, M. Skyllas-Kazacos, J. Power Sources 16 (1985) 85–95.
- [5] L.H. Thaller, in: 9th Intersociety Energy Conversion Engineering Conference, 1974, pp. 924–928.
- [6] H. Zhou, H. Zhang, P. Zhao, B. Yi, Electrochim. Acta 51 (2006) 6304–6312.
- [7] P. Lex, B. Jonshagen, Power Eng. J. 13 (1999) 142–148.
- [8] P. Han, H. Wang, Z. Liu, X. Chen, W. Ma, J. Yao, Y. Zhu, G. Cui, Carbon 49 (2011) 693–700.
- [9] M. Vynnycky, Energy 36 (2011) 2242–2256.
- [10] K. Knehr, E. Kumbur, Electrochem. Commun. 23 (2012) 76–79.
- [11] H. Zhang, H. Zhang, X. Li, Z. Mai, J. Zhang, Energy Environ. Sci. 4 (2011) 1676–1679.
- [12] H. Zhang, H. Zhang, X. Li, Z. Mai, W. Wei, Energy Environ. Sci. 5 (2012) 6299–6303.
- [13] C. Chen, H.K. Yeoh, M.H. Chakrabarti, Electrochim. Acta 120 (2014) 167–179.
- [14] A. Tang, J. Bao, M. Skyllas-Kazacos, J. Power Sources 248 (2014) 154–162.
- [15] H. Shen, X. Zhu, M. Shao, H. Cao, J. Appl. Math. 2013 (2013).
- [16] D. Aurbach, J. Power Sources 89 (2000) 206–218.
- [17] A.Z. Weber, J. Newman, Chem. Rev. 104 (2004) 4679–4726.
- [18] Q. Liu, G. Grim, A. Papandrew, A. Turhan, T. Zawodzinski, M. Mench, J. Electrochem. Soc. 159 (2012) A1246–A1252.
- [19] D. Aaron, Q. Liu, Z. Tang, G. Grim, A. Papandrew, A. Turhan, T. Zawodzinski, M. Mench, J. Power Sources 206 (2012) 450–453.
- [20] M. Moore, R.M. Counce, J. Watson, T.A. Zawodzinski, in: Meeting Abstracts, The Electrochemical Society, 2011, p. 2341.
- [21] M.L. Perry, R.M. Darling, R. Zaffou, ECS Trans. 53 (2013) 7–16.
- [22] M. Kazacos, M. Skyllas-Kazacos, J. Electrochem. Soc. 136 (1989) 2759–2760.
- [23] D. Aaron, Z. Tang, A.B. Papandrew, T.A. Zawodzinski, J. Appl. Electrochem. 41 (2011) 1175–1182.
- [24] K. Huang, X. Li, S. Liu, N. Tan, L. Chen, Renew. Energy 33 (2008) 186–192.
- [25] P. Zhao, H. Zhang, H. Zhou, J. Chen, S. Gao, B. Yi, J. Power Sources 162 (2006) 1416–1420.
- [26] M. Skyllas-Kazacos, G. Kazacos, G. Poon, H. Verseema, Int. J. Energy Res. 34 (2010) 182–189.